Rock strength characterization for excavations in brittle failing rock

B. H. Kim
MIRARCO-Mining Innovation, Geomechanics Research Centre, Sudbury, Canada

P. K. Kaiser
Centre for Excellence in Mining Innovation, Sudbury, Canada

ABSTRACT: The underground construction and mining industry are facing many geomechanics challenges. In mining, going deeper, increasing safety standards, and aiming for high productivity demands engineering to maximize value. In underground construction, geological complexities and mechanization demand better integration of engineering to ensure ease of construction. Rock under high stress tends to fail in brittle manner and a lack of engineering for constructability when tunneling in weak or brittle rock often leads to unnecessary delays and extra costs. Furthermore, brittle failing rock poses unique problems as stress-driven failure processes often dominate the tunnel behavior. In order to minimize the consequences of brittle failure, it is necessary to better understand the rock mass behavior rather than rock mass structure. This paper focuses on the aspect of rock strength determination for the engineering of deep excavations and presents a reinterpretation of laboratory test data for the estimation of rock strength at depth using an s-shape brittle failure criterion. It is found that intact rock strength from laboratory testing data may be underestimated if tests are not covering a sufficiently wide range of confinements.

1 INTRODUCTION

The determination of the rock strength is of significance for any stage in mining cycle, but it is most important at the pre-feasibility stage in order to scope realistic designs. Conventional system to characterize the rock mass strength have been established primarily from data related to tunnels at shallow to moderate depth (i.e., from 0 to about 1000 m). These parameters are then either used for support design, using empirical charts, again established based on experience at relatively shallow depths, or for selecting input parameters for numerical modeling.

It is hypothesized that the standard approach adopted to characterize the ground and to determine the rock strength properties at depth are flawed and generally tend to underestimate the rock strength and possibly the stiffness, particularly when the rock mass is characterized as massive to moderately jointed or blocky to very blocky. Theoretically, confining pressure dependent failure criteria, whether linear or non-linear, should incorporate the effect of increasing confinement and thus stress with depth, and in a perfect world most likely would. These criteria do tough imply that the failure mode remains the same, i.e., that shear failure occurs, However, highly confined rocks and rock masses may fail in a different manner than low confined rocks; for example, joints, particularly rough joints, may lock up, forcing failure through intact rock, the relative contribution to strength from rock joints and intact rock (rock bridges) may change, and the influence of heterogeneities promoting tensile failure components may also change.

It is therefore necessary to conclusively established that the hypothesis, that the rock strength in highly confined rocks is greater than generally anticipated, is actually valid and generally applicable, and then to develop new procedures to establish rock parameters that can be reliably used for the design of deep excavation.

2 THEORETICAL BACKGROUND

2.1 *Brittle rock failure envelopes*

Reliable estimates of the strength and deformation characteristics of rock masses are required for almost any form of analysis used for the design of slopes, foundations and underground excavations. Hoek and Brown (1980a, 1980b) proposed a method for obtaining estimates of the strength of jointed rock masses, based on an assessment of the interlocking of rock blocks and the condition of the surfaces between these blocks. This method was modified over the years in order to meet the needs of users who were applying it to problems that were not considered when the original criterion was developed (Hoek, 1983, Hoek and Brown, 1988).

Furthermore, comparisons of laboratory tests on very hard, brittle rocks were found to over-estimate the in situ rock mass strength. For example, laboratory tests and field studies on excellent quality Lac du Bonnet granite, reported by Martin and Chandler (1994), show that the in situ strength of this massive rock was significantly less that measured in the laboratory. This can be attributed, amongst other factors, to damage resulting from micro-cracking of the rock which initiates and develops critical intensities of cracks at lower stress levels in the field than in the laboratory on smaller, cylindrical specimens. Hence, when using the results of laboratory tests from these types of rocks to estimate the situ strength, it is prudent to consider processes of crack initiation, propagation and coalescence (Diederichs, 2003).

The failure of a laboratory specimen for example involves spalling due to long axial cracks at low confinements (Figure 1) or coalescence of small axial microcracks or lattice slip planes at higher confinements, to form a shear band (Hobbs et al. 1976).

In conventional usage, the Hoek-Brown and the Mohr-Coulomb strength envelopes assume that both cohesion and friction contribute to the peak strength, and that both strength components are mobilized instantaneously and simultaneously. This is certainly valid at high confinement levels, when the rock behaves in a ductile manner ($\sigma_1/\sigma_3 < 3.4$ according to Mogi (1966)) and cohesion and frictional strength components can be mobilized simultaneously. Diederichs (2003) suggests that this behavior results from the condition of all-around compressive strain at the point of crack initiation.

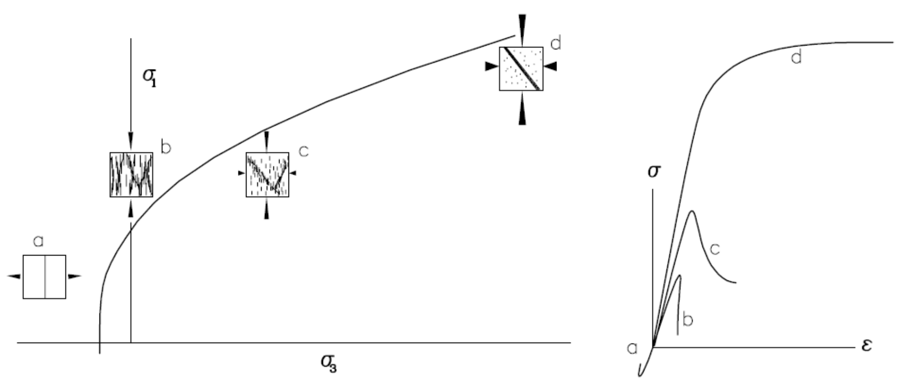

Figure 1. Effect of confinement on ultimate rupture mode: a) unstable Mode I crack extension in direct tension; b) quasi-stable Mode I spalling; c) dilational shear by coalescence of axial Mode I microcracks; d) non-dilational shear by coalescence of Mode II lattice slip planes under very high confinement (Diederichs 1999).

Martin (1994) and then Hajiabdolmajid *et al.* (2000) suggest that brittle strength mobilization can be reasonably represented as a two-stage process, with the pre-peak behavior governed by the cohesion of the rock, and the post-peak behavior by a strain-dependent adjustment of cohesive and frictional strength components, until, ultimately, the residual strength is dominated by the mobilized frictional strength within the damaged rock.

2.2 *Bi-linear envelope cut-off*

The strain dependent relationship between cohesion loss and friction mobilization has been demonstrated in stiff, sandy clays (Schmertman and Osterberg, 1968, Figure 2) and in granites by Martin (1994). Triaxial compression tests at different confinements were performed on samples of Kaolinite and graded sandy clay prepared at different pre-consolidation pressures. Based on the iso-strain contours, effective friction angles and apparent cohesion intercepts could be calculated as functions of axial strain for different pre-consolidation pressures. In the case of the Kaolinite, the initial friction, represented by ϕ, is minimal. Cohesive strength dominates at low strain. The friction in both soil materials gradually increases with inelastic strain. Cohesion on the other hand, is practically constant, for Kaolinite, over a large range of inelastic strain. This is consistent with the nature of cohesive clay bonding described earlier. For the sandy clay, however, the dense sand particles act as inhibitors to internal slip and create a brittle cohesional strength component more analogous to that in rock. This component of cohesion drops rapidly as the samples are strained and the frictional strength component is mobilized.

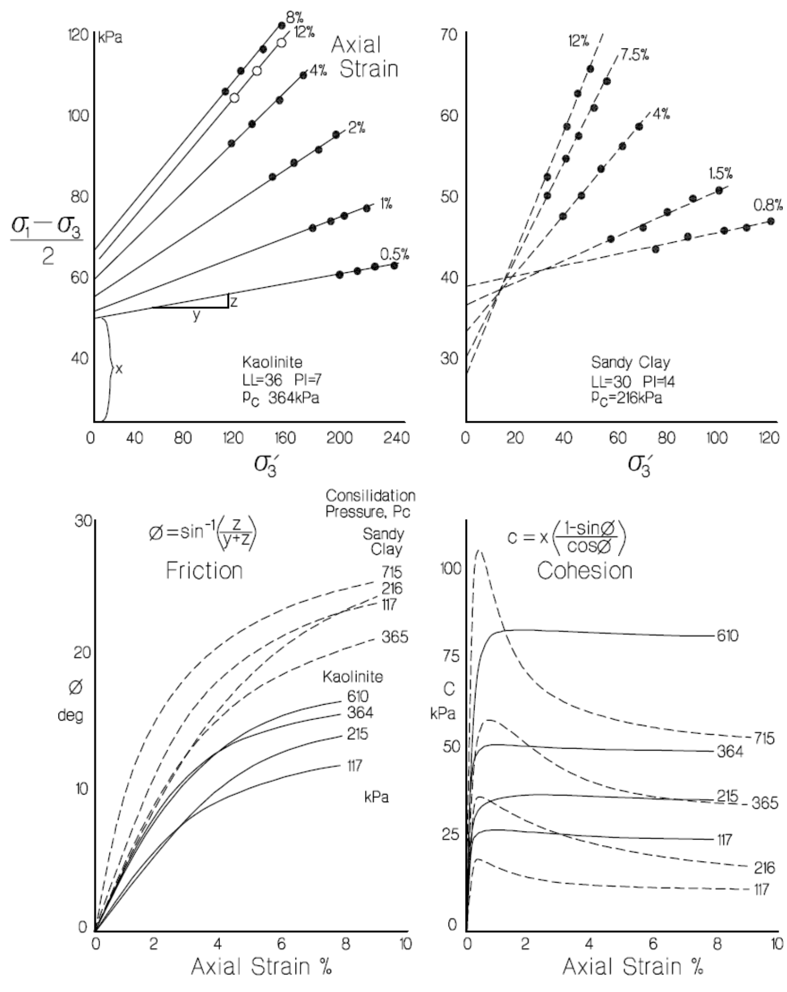

Figure 2. Cohesion loss and frictional strength mobilization in two saturated clays (Schmertman and Osterberg 1968, modified by Diederichs 1999)

At low confinement levels, the accumulation of rock damage, equivalent to loss of cohesion, typically occurs when the principal stress difference or deviator $(\sigma_1 - \sigma_3)$ = 0.33 to 0.5 *UCS* is reached or exceed. This is equivalent to a bi-linear failure cut-off starting at $\phi = 0$ (Mohr-Coulomb) or $m = 0$ (brittle Hoek-Brown) as discussed by Kaiser (1994) and Martin et al. (1999).

Below a damage threshold ($m = 0$), the rock is not damaged and remains undisturbed. When this threshold is exceeded, micro-seismicity is observed and damage accumulates, leading eventually to macro-scale shear failure if the confinement level is sufficiently high, preventing unstable crack or failure coalescence. The stress space, therefore, can be divided into four regions: no damage, spalling, shear failure and tensile failure zones.

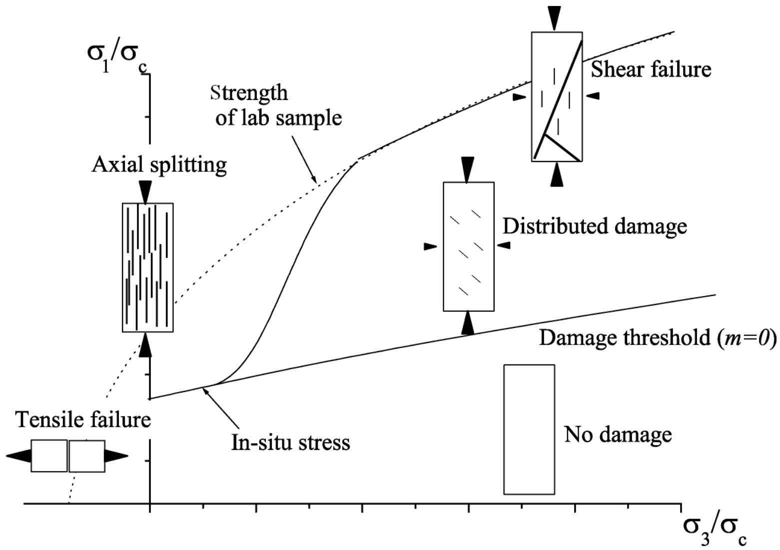

Figure 3. S-shape failure criteria showing damage threshold, spalling limit and rock mass strength envelope (after Kaiser et al. (2000); Diederichs (2003))

3 LIMITATIONS FOR APPLIACATION OF HOEK-BROWN FAILURE CRITERION

For intact rock pieces that make up the rock mass, the generalized Hoek-Brown failure criterion simplifies to:

$$\sigma_1 = \sigma_3 + \sigma_{ci}(m_i \frac{\sigma_3}{\sigma_{ci}} + 1)^a \tag{1}$$

The relationship between the principal stresses at failure for a given rock is defined by two constants, the uniaxial compressive strength σ_{ci} or *UCS* and a constant m_i. The third constant *a* is typically set to 0.5. Ideally, the values of these constants should be determined by statistical analysis of the results of a set of tensile, uniaxial and triaxial tests on carefully prepared core samples.

It is very important that the range of minor principal stress (σ_3) values over which these tests are carried out is at least half of uniaxial compressive strength. This means that tests must be conducted with the range of confinement up to 100 MPa if a uniaxial compressive strength is 200 MPa. Since such test equipment is rarely available, results are often interpreted using an insufficient confinement range. . In deriving the original values of σ_{ci} and m_i, Hoek and Brown (1997) used a range of $0 < \sigma_3 < 0.5\sigma_{ci}$ and, in order to be consistent, thus it is essential that the same range be used in laboratory triaxial testing for intact rock. At least five well spaced data points, and more for brittle rocks, should be included in the analysis.

Table 1 represents the uniaxial compressive strength σ_{ci} and the Hoek-Brown constant m_i for a quartzite calculated by the RocLab™ and a Hoek-Brown spreadsheet, respectively. This brittle, very friable quartzite is highly variable in strength at low confinements due to the effect of flaws and fissures at the sample scale. It is found that the values from the RocLab™ and the spreadsheet are very different even though the adopted calculation procedures are essentially identical. Figure 4 presents the triaxial test data and the Hoek-Brown failure envelope obtained by the spreadsheet and by RocLab™. The data sets are too scattered to be properly fitted by the Hoek-Brown failure envelope using RocLab™. The envelope is not extended to the whole range of the data set because the envelope is adjusted and re-generated considering a range of confinement, $0 < \sigma_3 < 0.5\sigma_{ci}$ (which due to the high scatter is lower and lower as the range is reduced). Furthermore, RocLab^{TM} limits the m_i value to 50. As a consequence, m_i is underestimated by RocLab^{TM}.

Table 1. Calculated uniaxial compressive strength σ_{ci} and the Hoek-Brown constant m_i by RocLab^{TM} (Rocscience, 2007) and the spreadsheet (Hoek, 2007), respectively.

	RocLab^{TM}	Spreadsheet
σ_{ci} (MPa)	86.0	57.7
m_i	50	108

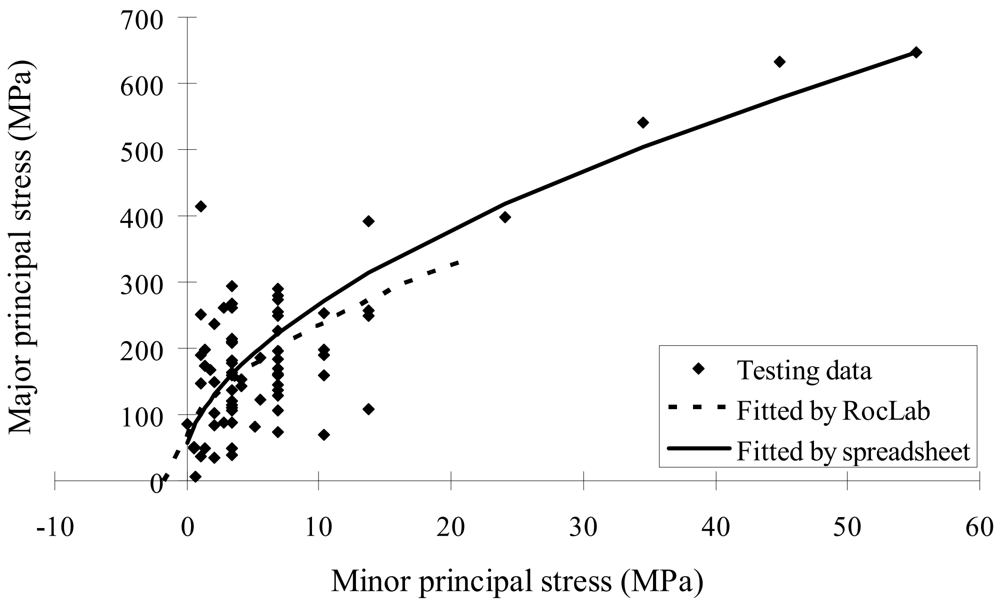

Figure 4. Example of interpretation of triaxial testing data for Quartzite fitted curve by both RocLab^{TM} and full range spreadsheet ($0 < \sigma_3 < 0.5\sigma_{ci}$)

The reason why this kind of problem occurs is that the results of RocLabTM are very sensitive to the range of confinement taken into account for a triaxial test. In other words, it is hard to trust a result from the RocLab^{TM} if a triaxial test is conducted in clear violation of the Hoek-Brown directives in terms of confinement conditions. Keeping the range of confinement, $0 < \sigma_3 < 0.5\sigma_{ci}$ is very important; however, if a rock is strong and its *UCS* is greater than 120MPa, it is technically difficult to fulfill this rule. Most triaxial test systems can only apply 60 to 70MPa or less.

Figure 5 shows the same triaxial test data and three Hoek-Brown envelopes with different m_i and *UCS* to fit the scattered data sets of the quartzite. The average *UCS* for this rock is 95MPa. Parameters for four approaches are listed in Table 2 and the corresponding non-linear envelopes are shown in Figure 4.

Table 2. Parameters for Hoek and Brown criterion shown in Figure 4

	Approach	*UCS* (MPa)	m_i
A	Average from *UCS* tests m_i from published rock type tables: $m_i = 23 \pm 3$ for Quartzite	95 (average)	26 (assumed)
B	RocLab™ applied to data from samples failing entirely through intact rock	225	26
C	Best fit to all data without RocLab™ constraint of $m_i \leq 50$ and average *UCS*	95	72

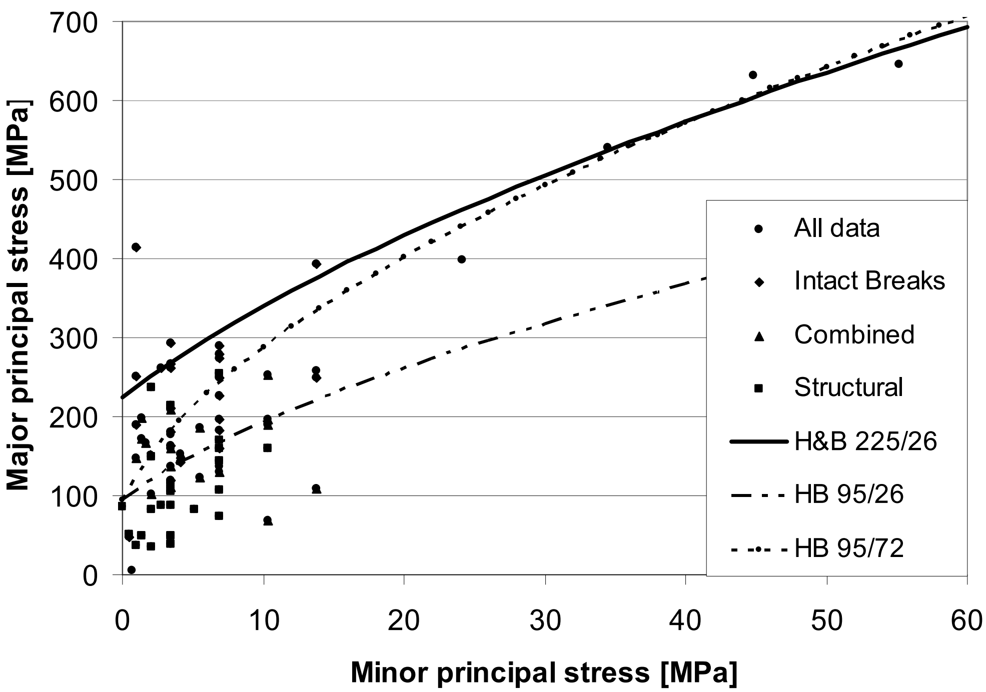

Figure 5. Triaxial test data for Quartzite with three fitted curves (with σ_{ci} and m_i values shown in legend)

The m_i value for Approach *C* is clearly out of range based on commonly recommended values for m_i and thus would be rejected. However, based on the above presented discussion, this unusually high m_i value of 72 best represents the entire data set. Approach *A* provides a best fit to the low confinement range (< 10MPa), though with a standard deviation of *UCS* of about 40 MPa, and approach *B* for the high confinement range (> 10MPa). Thus, it is obvious that calculation procedure for the parameter determination must be carefully selected and then defined for the applicable confinement range.

4 PROPOSED S-SHAPE BRITTLE FAILURE CRITERION

No matter how this data if fitted, it is evident that for brittle rocks a failure criterion is required that better describes the shape of the data. Both the Coulomb and the Hoek-Brown criterion assume a steady increase in strength with increasing confinement. More importantly, for both criteria it is implied that cohesive and frictional strength components are simultaneously mobilized. The data shown in Figure 5, however, suggests that there is a rapid transition from a wide scatter to a rather narrow scatters at about *UCS*/10 or σ_3 = 10 MPa.

Furthermore, ample evidence has been presented in the recent literature (Diederichs, 2003, Diederichs *et al*, 2004 and Diederichs *et al*, 2007) that support a bi-linear or bi-nonlinear shape of the failure envelope of rock in the low confinement zone.

Kaiser and Kim (2008a, 2008b) revisited Dr. Hoek's data base and showed that the rock strength was typically reduced to the left of a spalling limit of about $\sigma_1/\sigma_3 = 25$ to 20 (for intact rock) or typically for $\sigma_3 \leq UCS/10$ (Figure 6).

In order to express the behavior in the zone where crack propagation and spalling dominates and to reflect the transition from crack damage to shear failure, it is necessary to develop an s-shape criterion. The following Eqn (2) describes such an s-shape criterion:

$$\sigma_1 = k_2\sigma_3 + UCS_{II} + [\frac{(UCS_I - UCS_{II})}{1 + e^{(\sigma_3^{'} - \sigma_3^0)/\delta\sigma_3}}] \tag{2}$$

where, UCS_I is the unconfined compressive strength as determined in the laboratory, USC_{II} is the apparent *UCS*, obtained by linear back projection of a linear fit to high confinement data with slope k_2. The y-intercept at $\sigma_3 = 0$ represents the apparent uniaxial compressive strength (UCS_{II}) for the high confinement range or shear failure mode range. The other parameters are described below.

In Eqn (2), the lower intercept, UCS_I represents the intact unconfined rock strength as determined in the laboratory. The upper intercept, UCS_{II} represents an apparent unconfined intact rock strength that is appropriate to describe the strength of this rock during shear failure in the highly confined state (e.g., far away from an opening). The slope of the lower leg of the s-shape criterion k_1 is for now assumed to be equal to k_2 ($k_1 = k_2$).

The transition curve from spalling (lower confinement) to shear failure region (higher confinement) is called the spalling limit and is assume to start at the origin; thus with a slope $k_s .= \sigma_1 / \sigma_3$.

The remaining parameters are defined by Eqn (3) and (4), respectively.

$$\sigma_3^0 = \frac{(UCS_I - UCS_{II})}{2(k_s - k_2)} \tag{3}$$

$$\delta\sigma_3 = A\sigma_3^0 \ (A = 0.1 \sim 0.3) \tag{4}$$

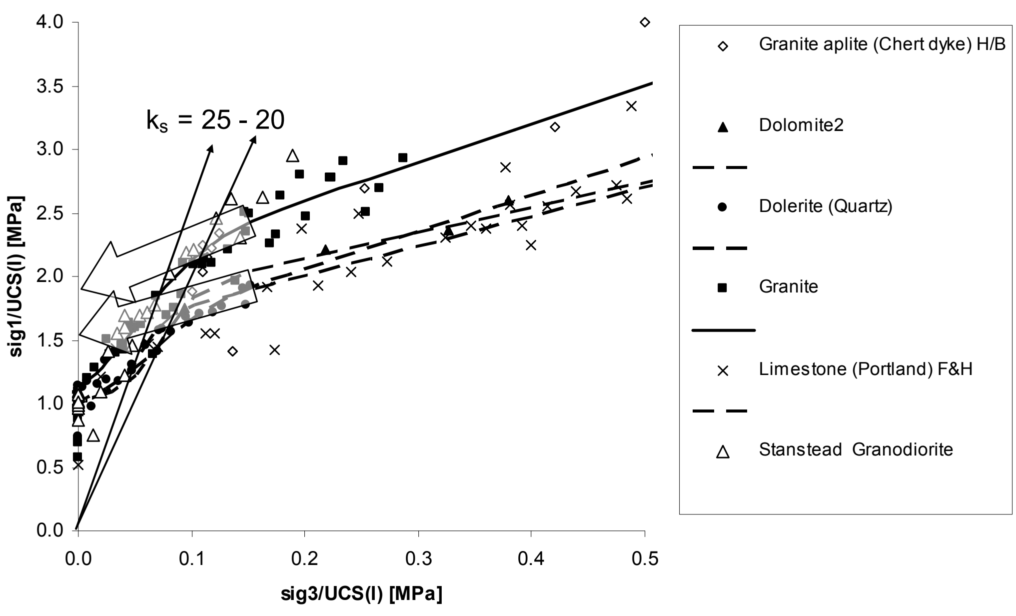

Figure 6. Laboratory test data of five rock types with similar behavior are grouped and fitted with s-shape failure criterion: (a) Granite Aplite, Granite, and Granodiorite (apparent $UCS_{II} = 1.8\ UCS_I$; $\phi = 35\text{-}37^o$; $k_s = 25$; and (b) Dolomite, Dolerite and Limestone (apparent $UCS_{II} = 1.55\ UCS_I$; $\phi = 23\text{-}25^o$; $k_s = 20$) (data courtesy: E. Hoek and J. Archibault; arrows point at apparent UCS_{II} for two rock types)

A procedure to interpret and fit triaxial testing data using the s-shape brittle failure criterion of Eqn (2) was developed. An approach to define the transition zone or spalling limit (between spalling and shear failure zone) is required. Microcracks are the source of a theory for brittle failure developed by Griffith (1924). The physical model underlying Griffith's theory is that microcracks are randomly distributed and oriented in the rock material. Under applied stress, failure occurs when vulnerably oriented microcrack extend due to tensile fracture propagation from the crack tips. Also, the Griffith crack theory suggests that microcrack propagation and thus rock mass damage is highly dependent on the confinement stress. This was shown by Hoek and Bieniawski (1965) when studying crack propagations in photo-elastic materials. The strong dependency of unstable crack propagation with confinement is illustrated by Figure 7. At low confinement, unstable tensile cracks propagation leads to their rapid coalescences which are reflected at the macro-scale by spalling. While standard failure criteria do consider the effect of confinement, it is speculated that the strength increase due to increasing confinement is generally underestimated by current failure criterion (e.g. Hoek-Brown criterion) in the low confinement range. Therefore, it is hypothesized that a domain of confinement stress between 0.02*UCS* and 0.1*UCS* represents the transition zone, and this was used for the results presented here.

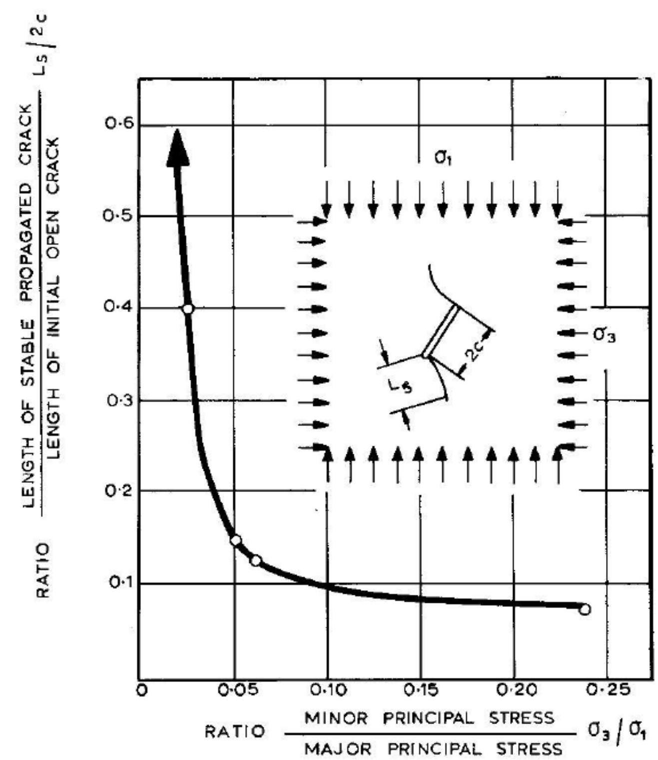

Figure 7. Relationship between stable crack length and ratio of applied principal stresses (Hoek and Bieniawski, 1965).

The adopted procedure to interpret and fit triaxial testing data to obtain an s-shape failure criterion is as follows. First, define a transition zone which confinement stress is from 0.02*UCS* and 0.1*UCS*. Now, a spalling zone which confinement less than 0.02*UCS*, and a shear zone with confinement stress greater than 0.1*UCS* is determined. Second, undertake a linear regression analysis of data sets in shear zone, thus k_2 and UCS_{II} are obtained as slope and y-intercept from the regression, respectively. The assumed physical process underlying this approach is that a cohesion intercept (UCS_{II}) with frictional shear failure, following the Coulomb criteria, properly describes highly confined rock when failing predominantly in shear.

The true UCS_I is determined as the mean value of *UCS* from lab testing, and k_s can be calculated as the slope if a best fit line to the data in the transition zone (through zero). This procedure was programmed in a spreadsheet and forms the basis for the results quoted below.

Figure 8 presents an example using test data for Sandstone Darley in Dr. Hoek's data base. In order to represent the variability the ±95 % confidence levels are plotted for the linear regression in the shear zone. It is seen that the data is very fitted by the s-shape failure criterion. The parameters of the corresponding s-shape failure envelop are shown in Table 3.

Table 3. Calculated parameters for s-shape failure criterion shown in Figure 8

UCS_I (MPa)	UCS_{II}/UCS_I	k_s	k_2
252.4	1.9	29	5.45

The parameters for data in a large data base of published test results (incl. Dr. Hoek's data) were determine in this manner.

Figure 9 shows that UCS_{II} is between 1 and 3-times the laboratory UCS_I or on average between 1.5 and 1.7 times higher than UCS_I. In other words, the apparent UCS_{II} for the rock strength in the highly confined zone (> ~*UCS*/10) is significantly greater than the *UCS* obtained in the laboratory.

From practical point of view, the rock strength in the core of pillar (under high confinement) is best described by UCS_{II} while the rock near an excavation at low confinement is best described by UCS_I. For rocks with distinct s-shape failure behavior, it is, therefore, more appropriate to consider the confinement range relevant for a given engineering problem before selecting design parameters. As a summary, UCS_I would be more relevant for support design, and UCS_{II} would be more suitable for pillar design.

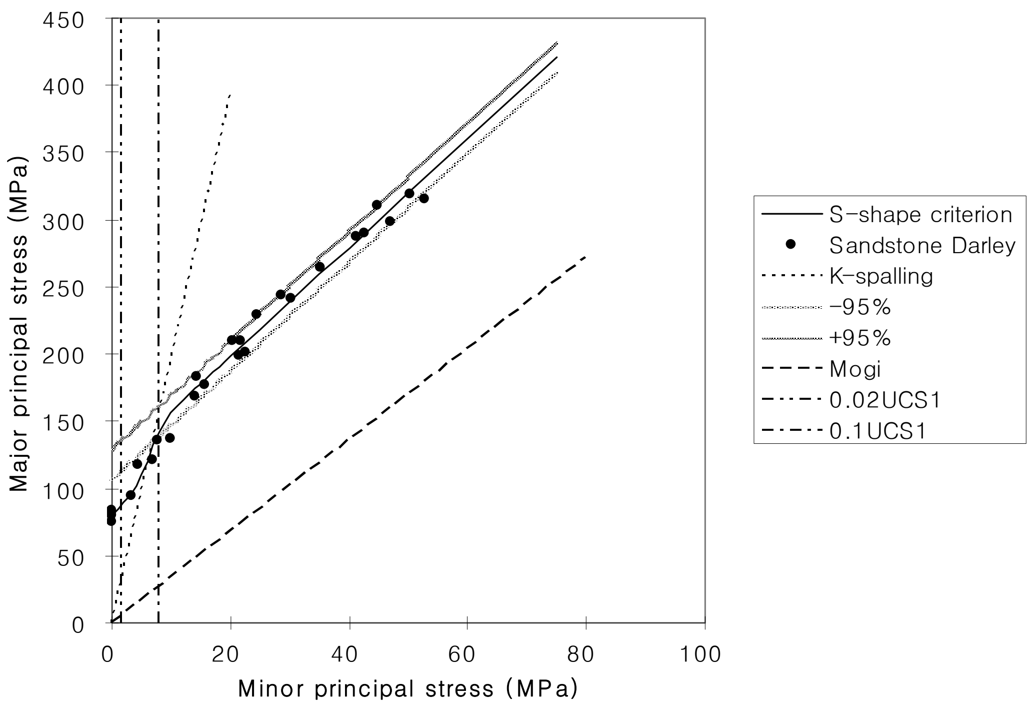

Figure 8. Result of fitting curve on s-shape criterion using the spreadsheet

The *UCS*-ratio obtained by fitting s-shape failure criterion to 54 rocks is presented in increasing order of brittleness in Figure 9. Almost all rock types in this set, from sedimentary rocks (coal, limestone, etc) to igneous and metamorphic rocks (granites, etc.), show some degree of brittleness.

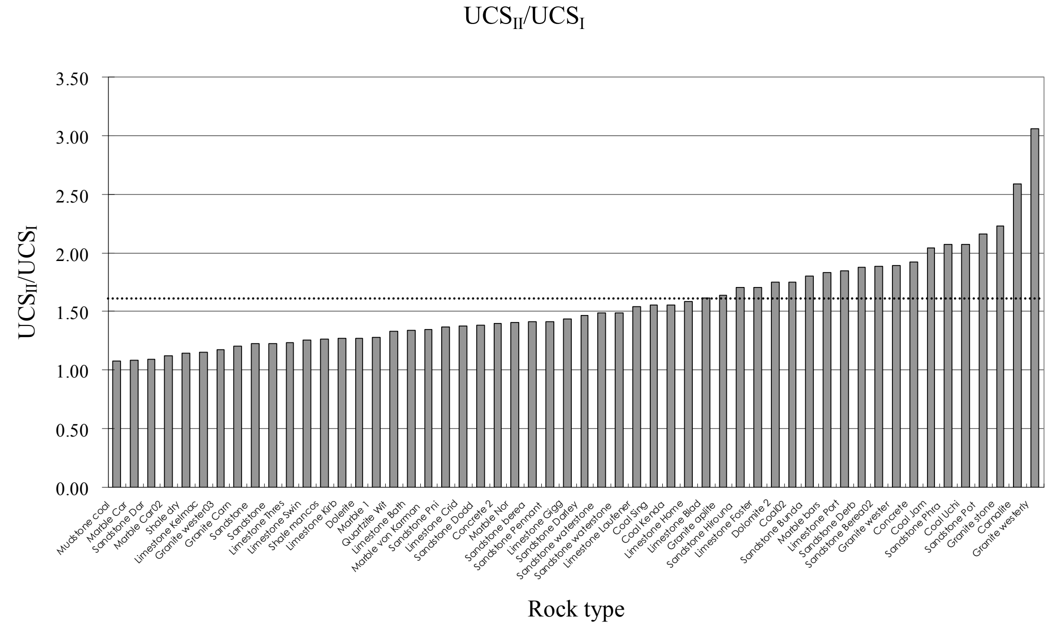

Figure 9. Calculated a ratio of UCS_{II} / UCS_I based on s-shape failure criterion for (mean: 1.56).

5 CONCLUSIONS

The underground construction and mining industry are facing many geomechanics challenges due to go deeper. In order to prevent or minimize unnecessary delays and costs, it is necessary to better anticipate when brittle rocks are to be encountered. The s-shape criterion allows assessing the degree of brittleness in terms of the *UCS*-ratio.

With respect to anticipating underground construction difficulties, it is most important to recognize that the rock and rock mass strength near the excavation which is represented as UCS_I may be significantly reduced for brittle failing rock. Hence, spalling, stain-bursting, and high potential for overbreak should be anticipated. On the other hand, extreme care must be taken when using measurements from the low confinement zone to determine confined rock parameters for pillar design due to the distinctly different behavior. The s-shape criterion identifies when such differences in rock behavior have to be anticipated.

From the results, it is found that the apparent *UCS* represented as UCS_{II} is on average 50 to 60% higher than UCS_I determined from laboratory test data. This is valid for a wide range of rock types. It is, therefore, suggested that the rock strength for the design of rock structure in confined and unconfined states, e.g. pillar under high confinement or near excavation at low confinement, should be obtained by fitting different regions of the s-shape criterion.

The same approach can be applied to rock mass strength data, but further work is required to establish procedures to degrade the s-shape envelopes for intact rocks to obtain the in situ rock mass strength.

Finally, this paper highlights that the blind application of RocLab™ or any corresponding regression analysis approach may produce mislead results and thus incorrect design parameters if the influence of brittle transition zone is not properly accounted for in the analysis. It is important to follow a systematic approach for laboratory data interpretation. Until procedures have been developed to consider the brittleness in designs, it is recommended that the strength be determined separately for the low and high confinement ranges.

6 PREFERENCES

Diederich, M.S. 1999. Instability of hard rock masses: The role of tensile damage and relaxation. *Ph.D. Thesis*, University of Waterloo.

Diederichs, M.S., Carvalho, J.L. and Carter, T.G. 2007. A modified approach for prediction of strength and post yield behaviour for high GSI rock masses in strong, brittle ground. *1st Canada-U.S. Rock Mech. Symp*., 249-257.

Diederichs, M.S., Kaiser, P.K. and Eberhard, K.E. 2004. Damage initiation and propagation in hard rock and influence of tunnelling induced stress rotation. *Int. J. Rock Mech. Min. Sci.*, 41: 785-812.

Diederichs, M.S. 2003. Rock fracture and collapse under low confinement conditions, Rocha Medal Recipient, *Rock Mech. Rock Engr.*, 36(5):339-381.

Griffith, A.A., 1924. Theory of rupture, *1st International Congress of Applied mechanics,* Technische Boekhandel and Drukkerij, Delft.

Hajiabdolmajid, V., Martin, C.D. and Kaiser, P.K. 2000. Modelling brittle failure, *4th North American Rock Mechanics Symp.* Seattle, Washington, A.A. Balkema, Rotterdam, 8p.

Hobbs, B.E., Means, W.D. Williams, Paul F. 1976. *An Outline of Structural Geology*. New York: John Wiley and Sons. 571p.

Hoek, E. 1983. Strength of jointed rock masses, 23rd. Rankine Lecture. *Géotechnique*, 33(3):187-223.

Hoek, E., 2007. *Practical rock engineering*, 2nd ed. Rocscience Inc.

Hoek, E., and Brown, E.T. 1980a. *Underground excavations in rock*. London: Instn Min. Metall.

Hoek, E. and Brown, E.T. 1980b. Empirical strength criterion for rock masses. *J. Geotech. Engng Div.*, ASCE 106(GT9), 1013-1035.

Hoek, E. and Brown, E.T. 1988. The Hoek-Brown failure criterion - a 1988 update., *15th Canadian Rock Mech. Symp.*, Toronto: Dept. Civ. Engineering, University of Toronto, 31-38.

Hoek, E. and Brown, E.T. 1997. Practical estimates of rock mass strength. *Int. J. Rock Mech. & Mining Sci. & Geomechanics Abstracts*. 34(8), 1165-1186.

Hoek, E. and Bieniawski, Z.T., 1965. Brittle rock fracture propagation in Rock under compression. *Int. J. Fracture Mechanics*, 1(3): 137-155.

Kaiser, P.K. 1994. Observational modelling approach for design of underground excavations. *SANGORM '94*, Pretoria: ISRM, 1-7.

Kaiser, P.K., Diederichs, M.S., Martin, C.D., Sharp, J. and Steiner, W. 2000. Underground works in hard rock tunnelling and mining. *GeoEng2000*, Technomic Publ. Co., 841-926.

Kaiser, P.K. and Kim, B.H., 2008a. Rock mechanics challenges in underground construction and mining, 1st *SHIRMS,* Perth, Australia, 23-38.

Kaiser. P.K. and Kim, B.H., 2008b. Rock mechanics advances for underground construction in civil engineering and mining, *KRMS 2008*, Chonnam National University, Gwangju, South Korea, 3-16.

Martin, C.D. 1994. The Strength of Massive Lac du Bonnet Granite around Underground Openings. *Ph.D. Thesis*. University of Manitoba.

Martin, C.D. and Chandler, N.A., 1994. The progressive fracture of Lac du Bonnet granite. *Int.. J. Rock Mech. & Mining Sci. & Geomechanics Abstracts*.31(6): 643-659.

Martin, C.D., Kaiser, P.K. and McCreath, D.R., 1999. Hoek-Brown parameters for predicting the depth of brittle failure around tunnels. *Can. Geotech. J*. 36, 136-151.

Mogi K. 1966. Pressure dependence of rock strength and transition from brittle fracture to ductile flow. *Bull. Earthquake Res. Inst. Japan*, 44, 215-232.

Schmertman, J.H. and Osterberg, J.O. 1968. An experimental study of the development of cohesion and friction with axial strain in saturated cohesive soils. *ASCE Research Conference on Shear Strength of Cohesive Soils*, 643p.

Rocscience Inc., 2007. *RocLab*, version 1.031.